Plant Cell Physiol. 48(9): 1243–1253 (2007)
doi:10.1093/pcp/pcm099, available online at www.pcp.oxfordjournals.org

Rapid paper

Location of a Possible miRNA Processing Site in SmD3/SmB Nuclear Bodies in Arabidopsis

Yoichiro Fujioka [1], Maki Utsumi [1], Yusuke Ohba [2] and Yuichiro Watanabe [1, *]

[1] *Department of Life Sciences, Graduate School of Arts and Sciences, University of Tokyo, Komaba 3-8-1, Meguro, Tokyo, 153-8902 Japan*
[2] *Laboratory of Pathophysiology and Signal Transduction, Department of Pathology, Hokkaido University Graduate School of Medicine, N15 W7, Kita-ku, Sapporo, 060-8638 Japan*

There has been much recent research on the contribution of microRNA (miRNA) in plant organogenesis and hormone action. In plants, it has been reported that Dicer-like 1 (DCL1), HYPONASTIC LEAVES1 (HYL1) and SERRATE (SE) are involved in the production of miRNAs. The means by which miRNAs are processed and transported is not well understood in detail, however. In this study, we investigated the intracellular localization and intermolecular interaction of these molecules using imaging techniques, including bimolecular fluorescence complementation and fluorescence resonance energy transfer techniques, making use of various enhanced fluorescent proteins. We found that DCL1, HYL1 and SE formed bodies which localized in the nuclei. We were also able to locate the miRNA primary transcript using an MS2-tagged method on these bodies. It appears very likely that the observed DCL1–HYL1–SE nuclear body is involved in miRNA production. Co-expression of SmD3 or SmB proteins revealed the localization of DCL1–HYL1–SE complexes in the SmD3/SmB nuclear bodies.

Keywords: Arabidopsis — Dicer-like 1 — HYL1 — Micro RNA — Processing — SERRATE.

Abbreviations: BiFC, bimolecular fluorescence complementation; CB, Cajal body; DCL1, DICER-LIKE 1; DEX, dexamethasone; dsRNA, double-stranded RNA; FRET, fluorescence resonance energy transfer; HA, hemagglutinin; HYL1, HYPONASTIC LEAVES1; miRNA, micro RNA; mRFP, monomeric red fluorescent protein; pre-miRNA, miRNA precursor; pri-miRNA, miRNA primary transcript; SE, SERRATE; SECFP, super-enhanced cyan fluorescent protein; siRNA, small interfering RNA; SmD3, small nuclear RNA-binding protein D3; YFP, yellow fluorescent protein.

Introduction

Micro-RNAs (miRNAs) are small, non-coding RNAs of 21–24 nucleotides which are produced after processing of single-stranded precursor RNAs with imperfect double-stranded stem–loops (Lim et al. 2003, Jones-Rhoades et al. 2006). They negatively regulate cognate complementary mRNAs at the post-transcriptional level by cleavage or by interference with translation. In animals, it has been shown that RNase III-like enzymes such as Drosha and Dicer are involved in miRNA biogenesis. It has been reported that these enzymes interact with certain double-stranded RNA- (dsRNA) binding proteins in order to function. DGCR8 or Pasha, together with Drosha, is essential in miRNA primary transcript (pri-miRNA) processing in mammals and *Drosophila* (Landthaler et al. 2004, Saito et al. 2005). R2D2 is required for loading of small interfering (siRNA) into the RNA-induced silencing complex (RISC) by interacting with Dicer-2 in *Drosophila* (Liu et al. 2006). In plants, it has been shown that Dicer-like (DCL1) protein catalyzes the maturation step from pri-miRNA (Park et al. 2002, Kurihara and Watanabe 2004). It has also been shown that HYPONASTIC LEAVES1 (HYL1), a dsRNA-binding protein, is part of a macromolecular complex and is involved in miRNA maturation (Lu and Fedoroff 2000). Recently, we and several other groups have demonstrated that DCL1 and HYL1 form a complex and that this association is important for the efficient and precise cleavage of pri-miRNA (Han et al. 2004, Vazquez et al. 2004, Kurihara et al. 2006). However, the biological significance of the association and the contribution of each component in processing is poorly understood.

Recently it has also been shown that SERRATE (SE), a C_2H_2 zinc finger protein unique to plant systems and without known homologs in animals, is critical for the accumulation of multiple miRNAs and the *trans*-acting small interfering RNA (ta-siRNA) (Yang et al. 2006). It has been demonstrated that SE also localizes in the nucleus and interacts physically with HYL1 (Yang et al. 2006).

In the current study, we used an in vivo imaging system to visualize the intracellular localization and possible interaction of the three components, DCL1, HYL1 and SE. Expression and localization of the proteins in planta were subsequently visualized after introduction mediated

*Corresponding author: E-mail, solan@bio.c.u-tokyo.ac.jp; Fax, +81-3-5454-6776.

by *Agrobacterium* into *Nicotiana benthamiana* leaves. Based on the success in detection of specific fluorescent signals, bimolecular fluorescence complementation (BiFC) (Hu and Kerppola 2003, Bracha-Drori et al. 2004, Walter et al. 2004, Citovsky et al. 2006) and fluorescence resonance energy transfer (FRET) (Dixit et al. 2006) techniques were applied to visualize the localization of and interactions among DCL1, HYL1 and SE, participants in miRNA processing. The results suggested that all three molecules form and co-localize in bodies which are located in nuclei. An MS2-tagged RNA-tracking system (Bi et al. 2006) was also applied to visualize the miRNA precursor molecule (pre-miRNA). Its localization on the bodies supported the involvement of the bodies in miRNA processing (Bertrand et al. 1998).

Results

Localization of individually expressed DCL1 and its derivative mutants, HYL1 and SE

In this study we focused on the behavior of DCL1, HYL1 and SE with regard to their role in miRNA processing. The localization of DCL1, HYL1 and SE has been reported in earlier publications (Han et al. 2004, Hiraguri et al. 2005, Yang et al. 2006) and also in a recent publication (Fang and Spector 2007) which appeared during preparation of this manuscript. To compare our system with earlier reports, we attempted to observe each protein, individually expressed, using an Agroinfiltration method. Other reports have used the protoplast or the onion epidermal system to determine the localization, but we used leaf tissues as we believed that this system reflects more natural conditions.

HYL1 and SE constructs, C-terminally fused with the variant of the yellow emitting mutant of green fluorescent protein (Venus) (Nagai et al. 2002), were expressed in leaves of *N. benthamiana* by Agroinfiltration. HYL1 (Fig. 1A, B) and SE (Fig. 1C, D) were mostly found in the nucleus and to a lesser extent in the cytoplasm. HYL1 and SE localization showed granules, or bodies, only in the nucleus. The results were consistent with earlier reports that used different host systems (Yang et al. 2006, Fang and Spector 2007, Song et al. 2007, Wu et al. 2007). No difference in localization of HYL1 or SE was observed between two translational constructs, N-terminally or C-terminally fused with Venus protein.

In preliminary experiments, in which we used the conventional cauliflower mosaic virus 35S promoter to direct the expression of each fusion protein, we did not observe fluorescence except when they were co-expressed with an RNA silencing suppressor, tomato bushy stunt virus p19 protein (Voinnet et al. 2003). Co-introduction of p19, however, often caused systemic necrosis in treated *N. benthamiana* leaves, and we therefore abandoned this strategy. Instead we used a dexamethasone (DEX)-inducible promoter vector in subsequent experiments to express DCL1, DCL1-7 and DCL1-9 constructs, N-terminally fused with Venus, in *N. benthamiana* leaves. Fluorescence was observed starting from 1 d after induction by DEX (Kurihara et al. 2006). Venus:DCL1 localized in the nucleus but not in the cytoplasm, and showed some bodies in the nucleus (Fig. 1E).

Previously we characterized and reported two DCL1 mutants, *dcl1-7* and *dcl1-9*, in miRNA maturation (Kurihara and Watanabe 2004). DCL1-7 protein has a point mutation (P415S) in the helicase domain, while DCL1-9 protein has a 74 amino acid truncation and an eight amino acid addition in the C-terminal second dsRNA-binding domain (Schauer et al. 2002). We were able to demonstrate the interaction of DCL1-7 protein with HYL1, but not that of DCL1-9 protein, by co-immunoprecipitation assay (Kurihara et al. 2006). Here we attempted to demonstrate the difference visually, using imaging techniques. The localization of Venus:DCL1-7 was similar to that of Venus:DCL1. It mainly localized in the nuclear bodies (Fig. 1F). This indicated that the point mutation in the helicase domain did not significantly affect the localization. However, Venus:DCL1-9 showed a different behavior, localizing in the nucleus but not in any bodies (Fig. 1G). It therefore appears that the second dsRNA-binding domain of DCL1, which is missing in DCL1-9, is important for the formation of, or localization in, the bodies. Whenever DCL1 and its mutants were observed, these proteins localized in the nuclear matrix to some extent, if not localized in certain bodies.

Immunodetection of the interaction between DCL1 and SERRATE

In previous work, we and other groups have shown interactions between DCL1 and HYL1 (Han et al. 2004. Kurihara and Watanabe 2004) and between HYL1 and SE (Yang et al. 2006) by co-immunoprecipitation. No reports have appeared, thus far, about the interaction between DCL1 and SE. We therefore attempted to detect the interaction between DCL1 and SE by co-immunoprecipitation before we performed BiFC and FRET analysis. Using the Agroinfiltration method (Kurihara et al. 2006), Y^C:DCL1 [tagged with hemagglutinin (HA)] and Y^N:SE (tagged with myc) proteins were transiently expressed in *N. benthamiana* leaves. When Y^C:DCL1 was immunoprecipitated with anti-HA antibody, Y^N:SE protein was co-precipitated, but Y^N alone was not (Fig. 2).

Interaction among DCL1, HYL1 and SE analyzed by BiFC analysis

We applied the BiFC system to analyze the intranuclear localization of and interaction among these molecules involved in miRNA processing.

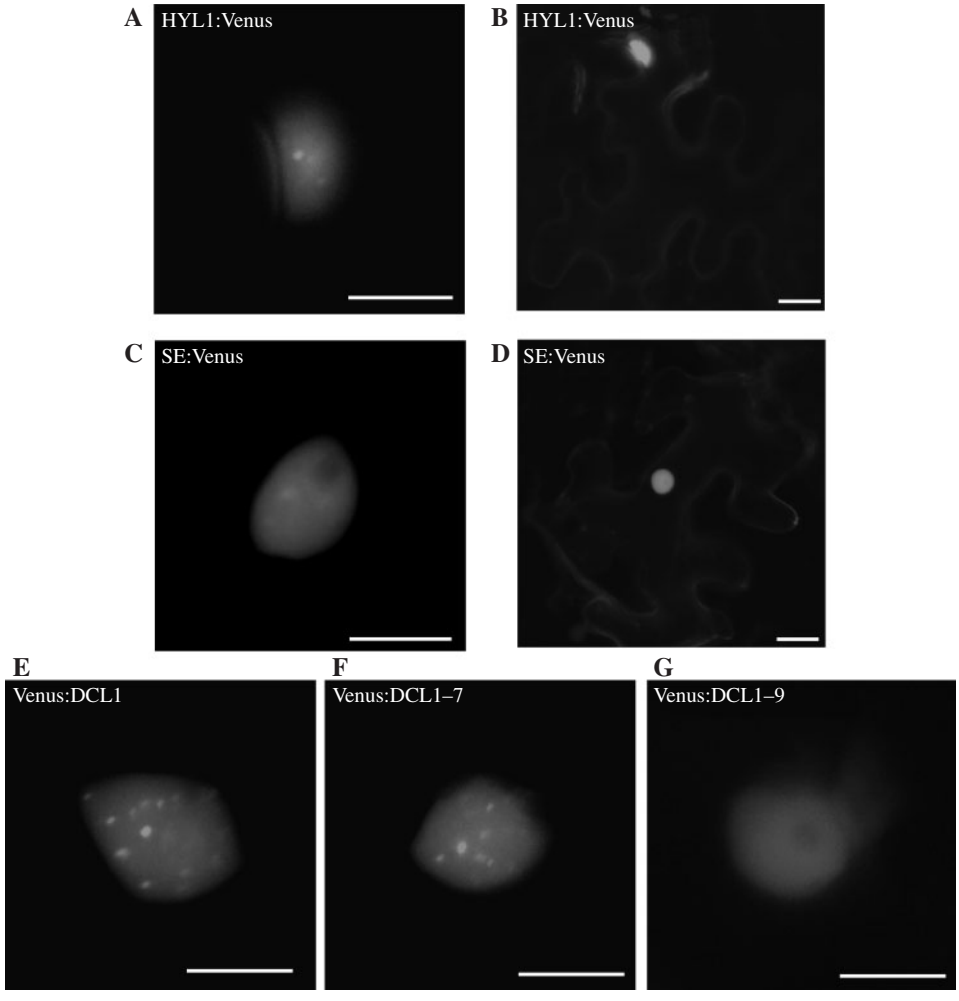

Fig. 1 Intranuclear distribution of HYL1, SE, DCL and its mutant form proteins. (A, B) HYL1:Venus; (C, D) SE:Venus; (E) Venus:DCL1; (F) Venus:DCL1-7; and (G) Venus:DCL1-9 were expressed in *N. benthamiana* leaves by Agrobacterium-mediated transient expression and observed under a fluorescent microscope after 48 h. Bars represent 10 μm.

DCL1 and SERRATE. The BiFC method was first applied to see the interaction between DCL1 and SE; BiFC fluorescence from Y^N:DCL1 and Y^C:SE was observed in the nuclear matrix and bodies (Fig. 3A-a). Many bodies were observed in the nucleus, as in the preliminary co-localization analysis (data not shown). The fluorescence in the bodies was more intense than that in the nuclear matrix. This implies that the interaction between DCL1 and SE is stronger in the bodies than in the matrix. It therefore appears that the bodies are the site of miRNA processing. The interaction between DCL1-7 and SE (Fig. 3A-b) was observed in some bodies, as with DCL1 and SE. Interestingly, DCL1-9 also interacted with SE and co-localized in a few nuclear bodies (Fig. 3A-c; Supplementary Table S4).

DCL1 and HYL1. The interaction between DCL1 and HYL1 was next tested by BiFC. When Y^N:DCL1 and Y^C:HYL1 were co-expressed in leaves of *N. benthamiana*, yellow fluorescence was observed in the nucleus (Fig. 3A-d). Similarly, an interaction between DCL1-7 and HYL1 was observed; DCL1-7 interacted with HYL1 in the nuclear bodies and matrix (Fig. 3A-e). BiFC fluorescence between DCL1-9 and HYL1 was detected only in the nuclear matrix, but not in the bodies (Fig. 3A-f; Supplementary Table S4).

HYL1 and SERRATE. When HYL1:Y^N and Y^C:SE were co-expressed in *N. benthamiana*, BiFC fluorescence was observed in the nuclear matrix and bodies (Fig. 3A-g; Supplementary Table S4). The interaction between HYL1 and SE was confirmed by this method. The HYL1–SE bodies were localized in nuclei.

DCL1, HYL1 and SE formed complexes and co-localized in nuclear bodies

The co-localization of the three molecules, DCL1, HYL1 and SE, was confirmed by the combination of BiFC and FRET analyses. When Y^N:HYL1, Y^C:SE

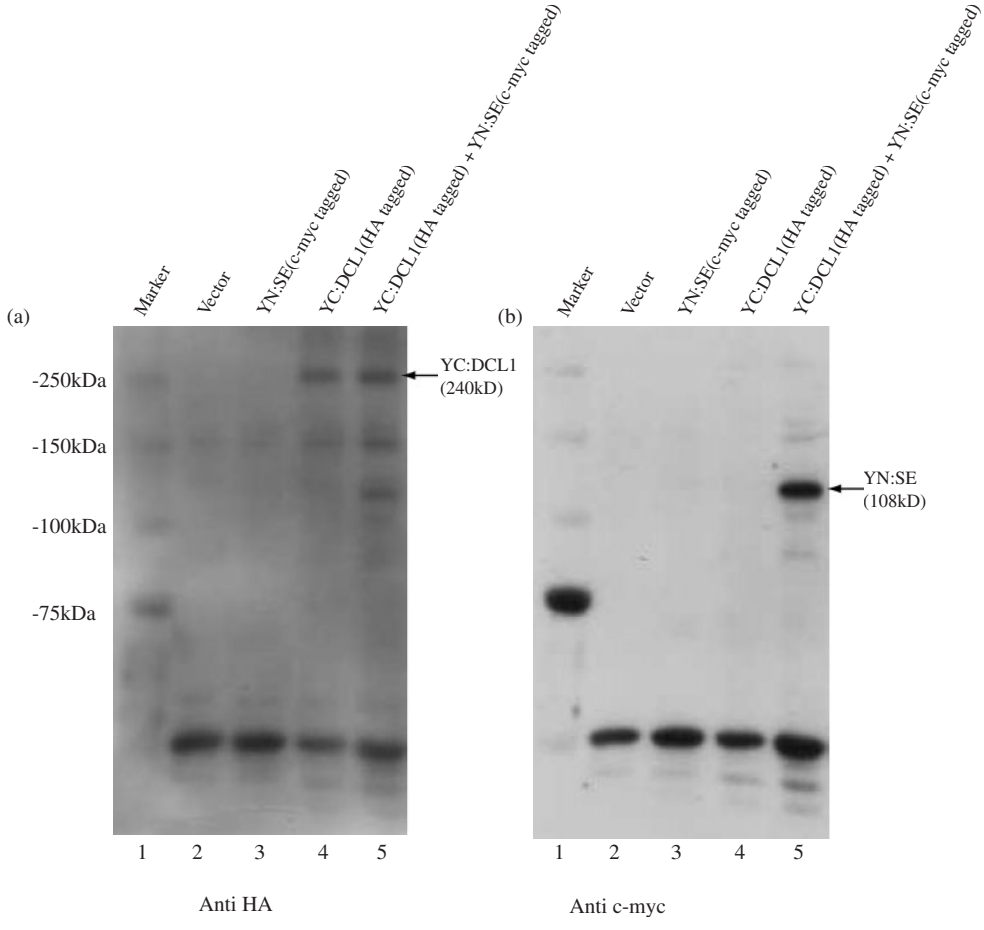

Fig. 2 Western blot analysis to detect the interaction between DCL1 and SE. Co-immunoprecipitation of Y^N:SE (tagged with the myc epitope) with Y^C:DCL1 (tagged with the HA epitope) using the anti-HA antibody. Lane 1: molecular mass markers; immunoprecipitates with anti-HA antibody from leaf extract agroinfiltrated with no insert vector (lane 2), Y^N:SE vector only (lane 3), Y^C:DCL1 vector only (lane 4), or both Y^N:SE and Y^C:DCL1 vectors (lane 5). Immunoprecipitates were analyzed by Western blot analysis with anti-HA (panel a) or anti-myc (panel b). It was shown that SE was co-immunoprecipitated with DCL1.

(Fig. 3B-a; yellow channel) and super-enhanced cyan fluorescent protein (SECFP):DCL1 (Fig. 3B-b; blue channel) were co-expressed in *N. benthamiana*, both images completely merged (Fig. 3B-c). It was suggested that the components of miRNA processing, DCL1, HYL1 and SE, are acting cooperatively in the same body structures in nuclei.

pri-miRNAs localized in the nuclear bodies (analysis by the MS2-tagged method)

Next, we applied FRET analysis to substantiate the BiFC data. Recently, the principle of FRET has been widely applied to analyze protein–protein interactions in living cells with spatiotemporal parameters. FRET analysis also consistently suggested that these three proteins co-localized in certain nuclear bodies (Supplementary Fig. S2) possibly involved in the processing of pri-miRNAs.

Thus, using two different imaging techniques, we were able consistently to demonstrate that DCL1, HYL1 and SE formed and localized in as yet uncharacterized nuclear bodies. We tried to obtain further supporting evidence that such bodies were actually involved in miRNA processing. To this end, we attempted to locate precursor molecules of miRNA inside cells to see whether they were actually trapped/located within such bodies.

The miR163 gene is found specifically in *Arabidopsis* (Allen et al. 2004). The matured form of miR163 accumulates at a high level in plants when compared with other miRNAs. miR163 could be used to trace the behavior of precursor molecules by efficient expression (Kurihara et al. 2006). In this case, it was advantageous for our analysis that miR163 is not found in *N. benthamiana*; when transiently introduced into *N. benthamiana* plants, the precursor molecules were properly transcribed and

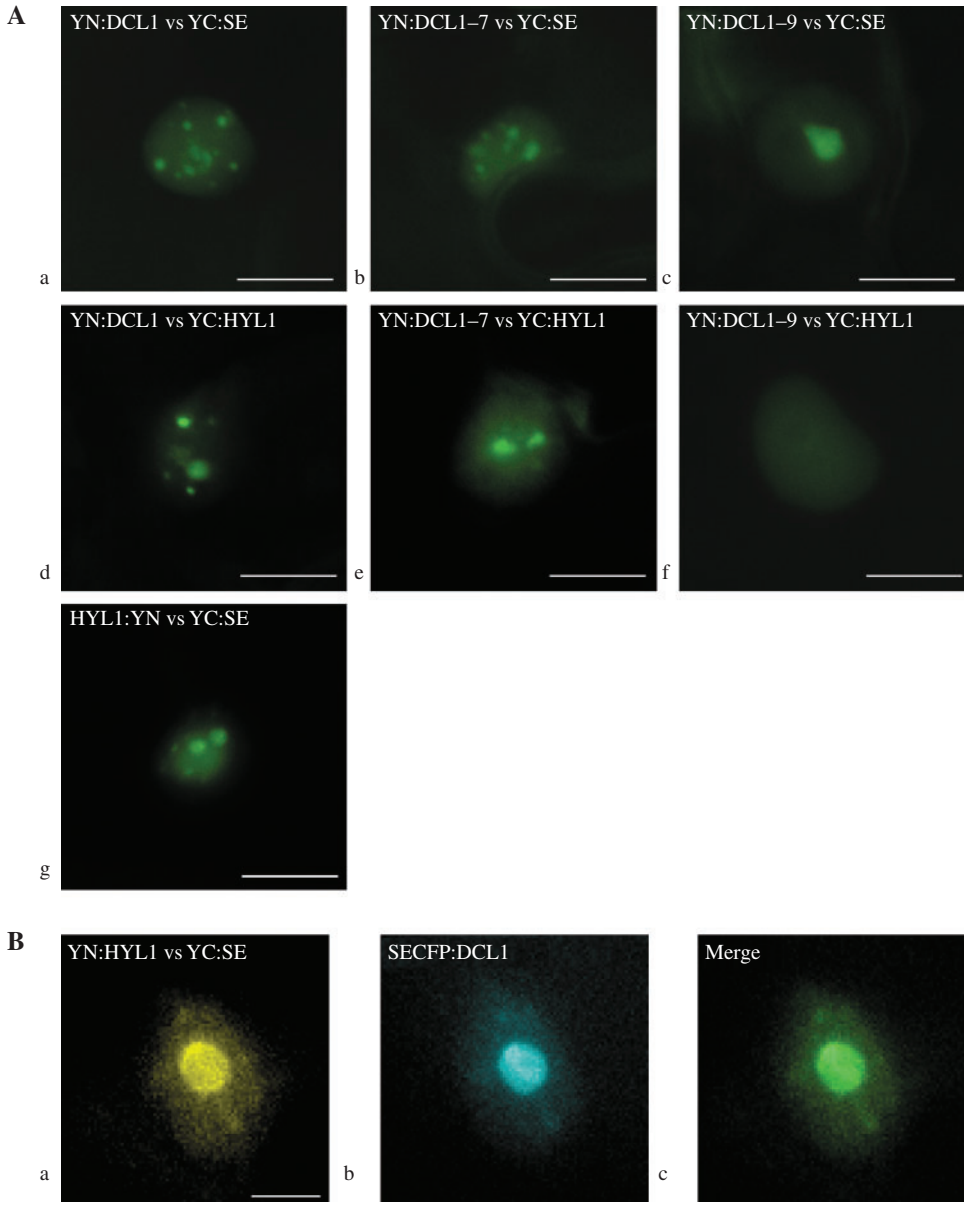

Fig. 3 (A) The intermolecular interactions and intranuclear localization detected by BiFC between a pair of DCL1s, HYL1 and SE. Y^C:SE and (a) Y^N:DCL1; (b) Y^N:DCL1-7; or (c) Y^N:DCL1-9 were co-expressed in the leaves of *N. benthamiana*. Likewise, Y^C:HYL1 was co-expressed concomitantly with Y^N:DCL1 (d); Y^N:DCL1-7 (e); or Y^N:DCL1-9 (f); and HYL1:Y^N with Y^C:SE (g). Fluorescent microscopic observation was performed 2 days after infiltration. Green signals indicate bimolecular interactions between the two molecules. (B) HYL1, SERRATE and DCL1 co-localize in intranuclear bodies. Y^N:HYL1,Y^C:SE and SECFP: DCL1 were co-expressed in leaves of *N. benthamiana*. (a) Yellow channel image: BiFC fluorescence of HYL1 and SE. (b) Blue channel image; CFP fluorescence of DCL1. (c) Merged image. Indication of co-localization of HYL-SE and DCL1. Bars represent 10 μm.

processed to mature miR163 in this heterologous system (Kurihara et al. 2006).

Based on this background, we attempted to visualize pri-miR163 RNA by an MS2-tagged RNA-tracking system (Bertrand et al. 1998). The MS2 coat protein gene was translationally fused with Venus protein (CP_{MS2}:Venus) and singly introduced into *N. benthamiana* plants. In the absence of pri-miRNAs, we were able to see fluorescence of CP_{MS2}:Venus in the cytoplasm and nucleus, but no bodies in the nucleus. (Fig. 4A). In contrast, when the pri-miRNA construct (pri-miR163:MS2 6×-pTA7002) was co-introduced, many bright bodies were observed in the nucleus (Fig. 4B). This confirmed that pri-miRNAs were localized in these naturally occurring bodies. When we

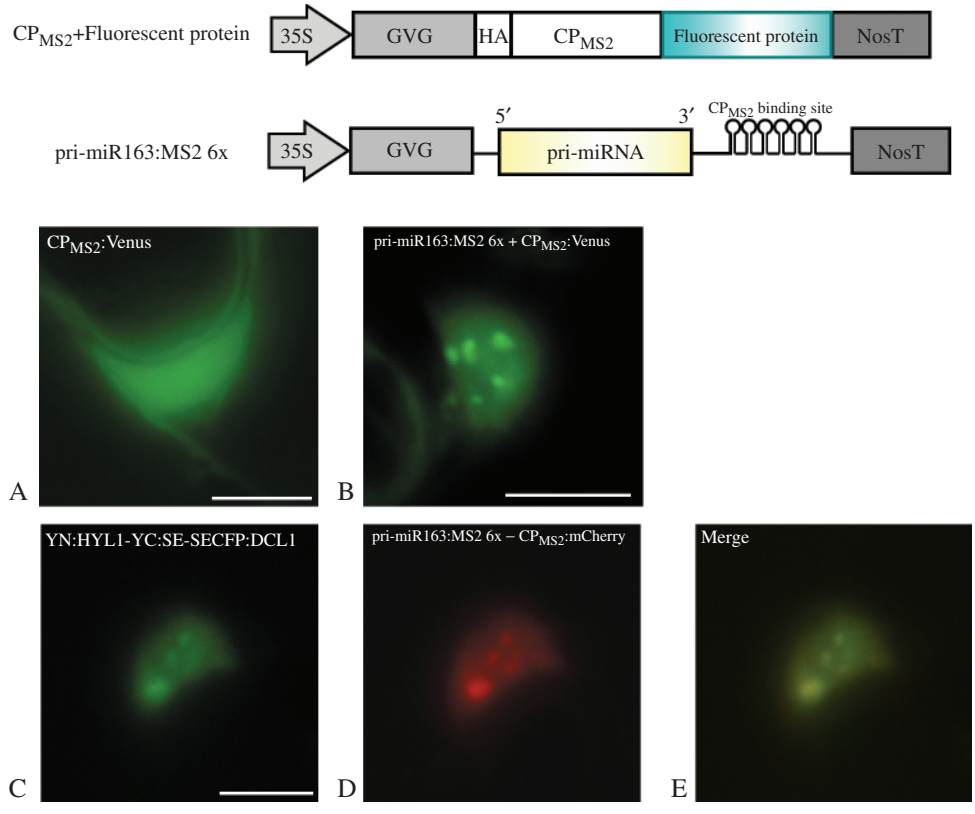

Fig. 4 An intranuclear DCL1–HYL1–SE body contains pri-miRNA. CP_{MS2}:Venus was co-expressed alone (A) or with pri-miR163:MS2-6× (B) in leaves of *N. benthamiana* and observed 2 days after introduction. Pri-miR163 co-localized on nuclear bodies that were similar to DCL1–HYL1–SE bodies. Next, CP_{MS2}:mCherry was co-expressed with Y^N:HYL1, Y^C:SE, SECFP:DCL1 and pri-miR163:MS2-6× in leaves of *N. benthamiana*. Confocal images of Y^N:HYL1, Y^C:SE and SECFP:DCL1 (C) and CP_{MS2}:mCherry (D). (E) is a merged image of (C) and (D). Bars represent 10 μm.

observed DCL1, HYL1 or SE, images of bodies were almost identical to those of pri-miRNAs.

We attempted to verify whether the pri-miR163 bodies were identical to DCL1, HYL1 and SE bodies. To do this, we co-introduced constructs of CP_{MS2}:mCherry as pri-miRNA probe, and the four components of miRNA biogenesis, pri-miR163:MS2 6×-pTA7002, Y^N:SE, Y^C:HYL1 and SECFP:DCL1. The bodies, which were revealed by DCL1/HYL1/SE and pri-miR163, fluoresced well in green (Fig. 4C) and red (Fig. 4D). Both images merged well in yellow, indicating co-localization (Fig. 4E).

Almost all bodies where DCL1, HYL1 and SE co-localized contained pri-miRNA. Thus it was very likely that such bodies normally existed in the nucleus and were not formed adventitiously due to introduction of exogenous genes. They are possibly involved in miRNA maturation.

Intranuclear localization of the bodies

In plants, nuclear subdomains have not yet been well characterized. Among them, rather exceptionally, the nucleolus and Cajal body (CB) have been characterized and described to some extent (Shaw and Brown 2004, Collier et al. 2006, Li et al. 2006). As above, it was observed that DCL1–HYL1–SE bodies were associated with nucleoli or bodies similar to CBs. Thus, we aimed to check whether such miRNA processing bodies were identical to, or encompassed in, nucleoli or CBs.

Nucleolin is one of the most abundant proteins in the nucleolus and is a multifunctional protein involved in several steps of ribosome biogenesis. In *Arabidopsis thaliana*, nucleolin-like protein AtNUC-L2 is a homolog of human and yeast nucleolin, and localizes in the nucleolus (Pontvianne et al. 2007). Under fluorescent microscopy, AtNUC-L2 visualized the nucleolus in *N. benthamiana*. When Y^N:HYL1 and Y^C:DCL1, Y^N:HYL1 and Y^C:SE, or Y^N:SE and Y^C:DCL1 were co-expressed with nucleolin, some bodies localized close to nucleolin, but did not merge (Fig. 5A–C; Supplementary Table S5).

CBs are frequently associated with the nucleolus (Shaw and Brown 2004). SmD3 is recognized as the marker protein of CBs (Li et al. 2006); we constructed SmD3, fused C-terminally with mCherry fluorescent protein

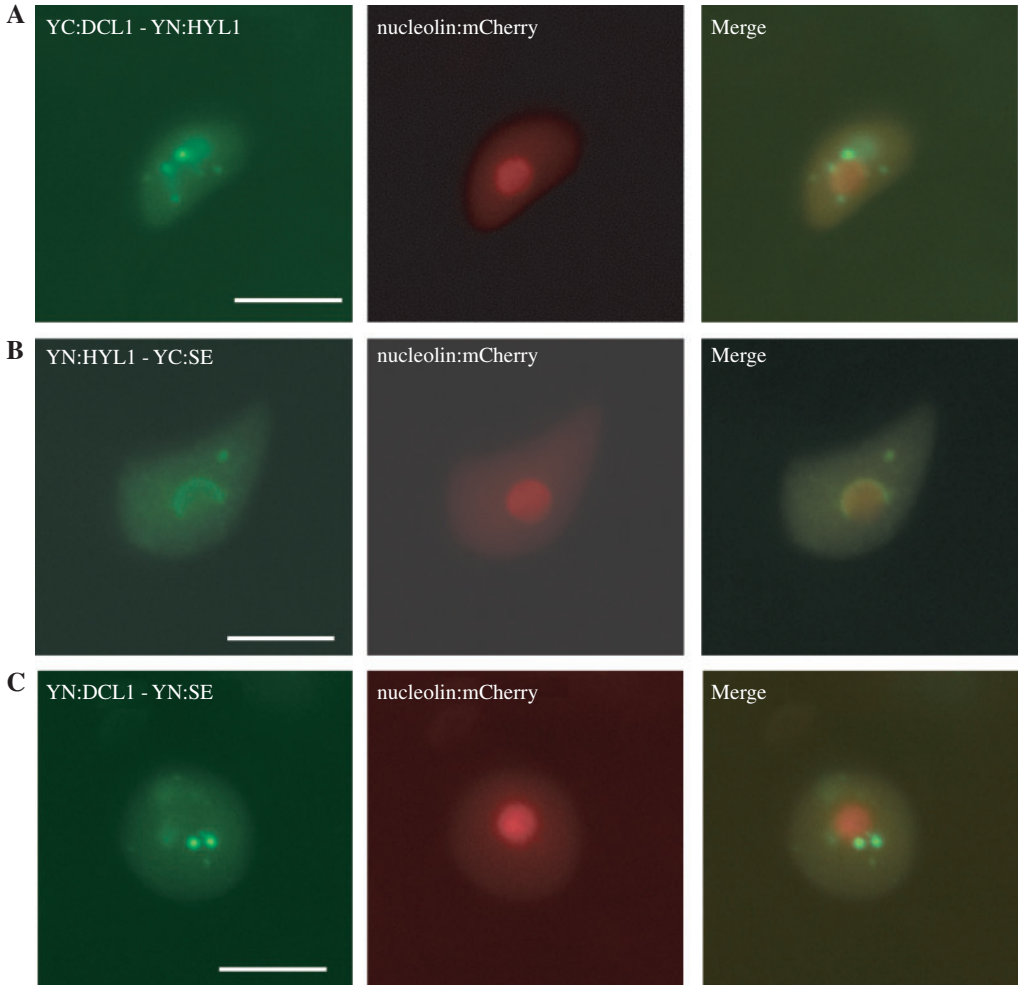

Fig. 5 miRNA processing bodies are located close to but are distinct from nucleoli. Nucleolin:mCherry was co-expressed with Y^C:DCL1 and Y^N:HYL1 (A), Y^C:HYL1 and Y^N:SE (B) and Y^C:DCL1 and Y^N:SE (C) in leaves of *N. benthamiana* and observed. Bars represent 10 μm.

(Shaner et al. 2004), and observed whether DCL1–HYL1–SE bodies were localized in, or on, CBs.

When Y^C:DCL1 and Y^N:HYL1 were co-expressed with SmD3:mCherry in *N. benthamiana*, most DCL1–HYL1 fluorescence co-localized in the SmD3 bodies (Fig. 6A). When Y^N:SE and Y^C:HYL1 were co-expressed with SmD3:mCherry, SE–HYL1 fluorescence overlapped with SmD3 bodies (Fig. 6B). When Y^C:DCL1 and Y^N:SE were co-expressed with SmD3:mCherry, most DCL1–SE fluorescence overlapped again with SmD3 bodies (Fig. 6C; Supplementary Table S6). These results imply that DCL1–HYL1–SE complexes are formed in the SmD3 bodies.

Furthermore, we also tested another marker protein of CBs, SmB (Li et al. 2006), for co-localization analysis. We constructed SmB fused C-terminally with mCherry. When Y^C:DCL1 and Y^N:HYL1, Y^N:SE and Y^C:HYL1, or Y^C:DCL1 and Y^N:SE were co-expressed with SmB:mCherry in *N. benthamiana*, most fluorescence co-localized in the SmB bodies (Fig. 6D–F; Supplementary Table S6).

We showed that DCL1–HYL1, HYL1–SE and DCL1–SE complexes co-localized with SmB. These results confirmed that DCL1–HYL1–SE was located in bodies formed by SmD3 or SmB, possibly assigned as CBs.

On the other hand, we tested another CB marker protein, coilin (Shaw and Brown 2004). When Y^C:DCL1 and Y^N:HYL1, Y^N:SE and Y^C:HYL1, or Y^C:DCL1 and Y^N:SE were co-expressed with coilin:mCherry, bodies did not merge well with those of coilin (Fig. 6G–I; Supplementary Table S6). This indicates that DCL1–HYL1–SE complexes did not localize in bodies which were formed by coilin.

When SmD3:Venus was co-expressed with SmB:mCherry, they co-localized in the nuclear bodies which are CBs (Supplementary Fig. S3A). In contrast,

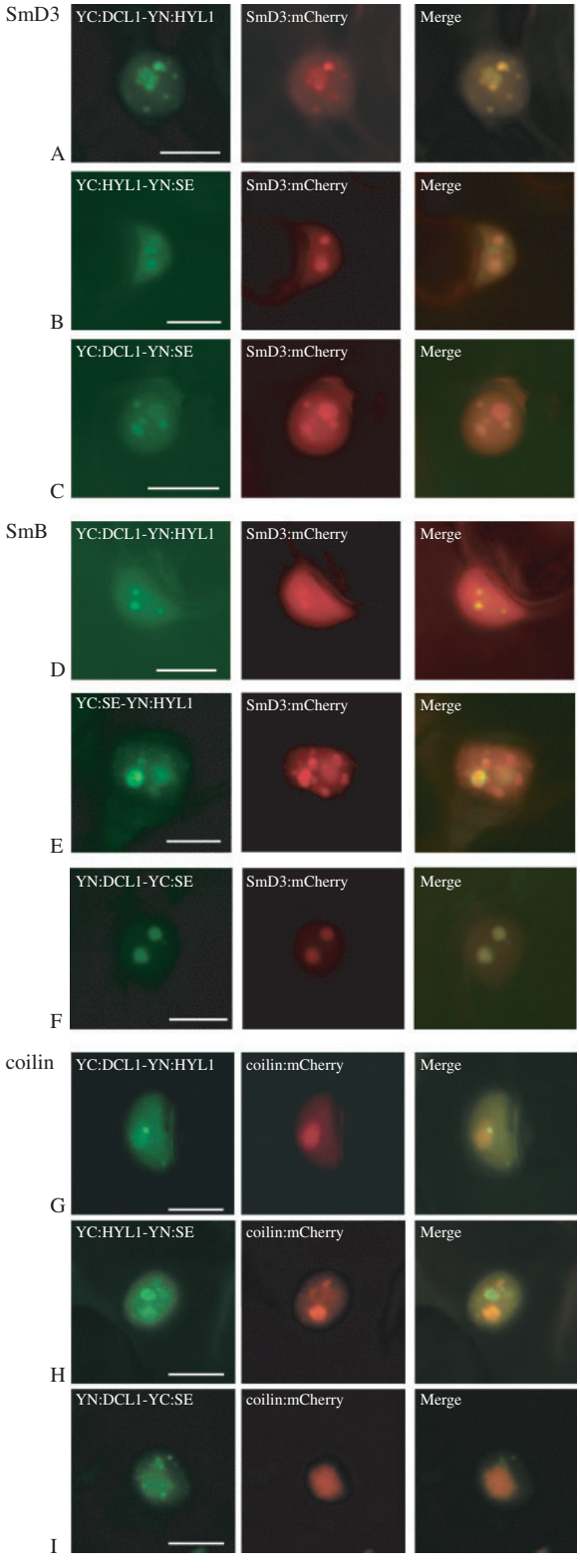

Fig. 6 miRNA processing bodies are located in the SmD3/SmB bodies. SmD3:mCherry was co-expressed with Y^C:DCL1 and Y^N:HYL1 (A), Y^C:HYL1 and Y^N:SE (B) and Y^C:DCL1 and Y^N:SE (C) in leaves of *N. benthamiana* and observed. SmB:mCherry was co-expressed with Y^C:DCL1 and Y^N:HYL1 (D), Y^N:HYL1 and Y^C:SE (E) and Y^N:DCL1 and Y^C:SE (F). Coilin:mCherry was co-expressed with Y^C:DCL1 and Y^N:HYL1 (G), Y^C:HYL1 and Y^N:SE (H) and Y^N:DCL1 and Y^C:SE (I). Bars represent 10 μm.

when SmD3:mCherry or SmB:mCherry was co-expressed with coilin:Venus, they did not merge well (Supplementary Fig. S3B, C). These results imply that CBs are of at least two types; one is formed by SmD3/SmB and another by coilin. Considering these results, we presumed that DCL1–HYL1–SE localized in CBs which were formed by SmD3/SmB.

Discussion

DCL1, HYL1 and SE are organizing miRNA processing bodies in nuclei

In a previous study we investigated the involvement of DCL1 and HYL1 in miRNA processing of pri-miRNA and pre-miRNA. We showed that both proteins are involved in precise and efficient cleavage of the precursor stem–loop structured RNA into mature miRNA (Kurihara and Watanabe 2004, Kurihara et al. 2006). We also found evidence that the interaction between the two proteins is positively involved in the cleavage (Kurihara et al. 2006).

Recently it was reported that another protein, SE, is also involved in miRNA processing and contributes to normal plant development along with DCL1 and HYL1 (Yang et al. 2006).

In this study we were interested in whether DCL1, HYL1 and SE interact with each other to form or to localize in a certain body. Using BiFC (Figs. 3, 4) and FRET (Supplementary Fig. S2) techniques, we were able consistently to observe in vivo images of the interaction between these molecules and the possible resulting bodies. Furthermore, when we applied an MS2-tagged system, we found that the bodies contained the miRNA precursor molecules, strongly indicating that the body is actually involved in miRNA processing.

DCL1–HYL1–SE bodies are associated with the Cajal body marker SmD3, but not with coilin

We constructed SmD3 or SmB fused, C-terminally, with mCherry fluorescent protein (Shaner et al. 2004), to see the relationship with the CB. When Y^C:DCL1 and Y^N:HYL1, Y^N:SE and Y^C:HYL1, or Y^C:DCL1 and Y^N:SE were co-expressed with SmD3:mCherry in *N. benthamiana*, all sets of both proteins co-localized in SmD3/SmB bodies (Fig. 6A–F; Supplementary Table S6).

On the other hand, we tested another CB marker protein, coilin (Shaw and Brown 2004). When Y^C:DCL1 and Y^N:HYL1, Y^N:SE and Y^C:HYL1, or Y^C:DCL1 and Y^N:SE were co-expressed with coilin:mCherry, each body did not merge well with those of coilin (Fig. 6G–I;

Supplementary Table S6). Recently, during preparation of this manuscript it was reported that HYL1 did not localize in CBs which were marked by coilin in *Arabidopsis* protoplasts (Song et al. 2007). Our data were not contradictory to those of that study. Our observation is also consistent with another report that nuclear dicing bodies (D-bodies) differ from coilin CBs (Fang and Spector, 2007). Using the other known SmD3 and SmB markers, the possible miRNA processing bodies were found to be closely similar or identical to CBs, where SmD3 and SmB localized but coilin did not (Fig. 6, Supplementary Fig. S3, Supplementary Table S6). Thus we could not exclude the involvement of CBs in miRNA processing like recent reports. Also it became a lesson that we might have drawn a different conclusion regarding CBs if we had depended totally on a single molecular marker.

Supplementary Fig. S3 showed that fluorescent signals of coilin were detected in more restricted regions than those of SmD3 and SmB. Several observations gave similar results, but we could not make a definitive conclusion as to whether coilin CBs were smaller than SmD3/SmB CBs.

It is recognized that CBs serve as centers for the maturation, processing and recycling of several ribonucleoparticles (Shaw and Brown 2004, Cioce and Lamond 2005). Recently it was also proposed that the CB plays a role in the processing of transcripts during the early steps of RNA interference (RNAi) and the incorporation of the siRNA products into an AGO4/NRPD1b/siRNA ribonucleoprotein complex that is recruited for RNA-directed DNA methylation at target loci (Li et al. 2006). Now that the DCL1–HYL1–SE complexes also appear to be located in these SmD3/SmB CBs, we need to determine if the machinery for RNA-directed DNA methylation and that for miRNA production are co-localized. If this is the case, orchestration of the two pathways should be systemically conducted in the SmD3/SmB CBs.

Materials and Methods

Construction of expression vectors

The plasmid, TA7002 (Aoyama and Chua 1997), was used as the transient expression system throughout this work.

Plasmids for FRET analysis

We introduced the Gateway system (Invitrogen, Carlsbad, CA, USA) into pTA plasmids and placed Venus (Nagai et al. 2002), SECFP (Sawano and Miyawaki 2000) or mCherry (Shaner et al. 2004) coding sequences just downstream or upstream of the cloning site. When we placed the protein coding region in the site of Venus-pTA7002^{GW}(N), SECFP-pTA7002^{GW}(N) or mCherry-pTA7002^{GW}(N), we were able to obtain proteins C-terminally fused with the respective fluorescent proteins. When we used Venus-pTA7002^{GW}(C), SECFP-pTA7002^{GW}(C) or mCherry-pTA7002^{GW}(C), we obtained proteins N-terminally fused with the respective fluorescent proteins. To eliminate the possibility of unfavorable protein structures caused by N- or C-terminal fusion, we attempted to construct every possible fusion (see the Supplementary Fig. S1 for diagrams of plasmid constructions).

Plasmids for BiFC analysis (Walter et al. 2004)

We constructed four types of BiFC vectors to express N-terminally or C-terminally fused proteins, with N-half or C-half yellow fluorescent proteins (YFPs) for each test protein, by placing the cDNA fragment using the Gateway system into the following four plasmids: pYN7002^{GW}, pYC7002^{GW}, p7002YN^{GW} and p7002YC^{GW}. When the DCL1 cDNA fragment was inserted into pYN7002^{GW} or pYC7002^{GW}, the N- or C-terminal fragment of YFP was bridged by the c-myc or HA epitope peptide, and C-terminally fused with DCL1. The expressed fusion protein was designated as Y^{N}:DCL1 or Y^{C}:DCL1, respectively. When the DCL1 cDNA fragment was inserted into p7002YN^{GW} or p7002YC^{GW}, the N- or C-terminal fragment of YFP was bridged by the c-myc or HA epitope peptide, and N-terminally fused with DCL1, and the expressed fusion protein was designated as DCL1:Y^{N} or DCL1:Y^{C}, respectively. Likewise, the corresponding plasmids of HYL1 and SE were constructed and fusion proteins were designated in the same way. Plasmids are listed in Supplementary Table S1.

Plasmids for the MS-2 tagged method (Bertrand et al. 1998; Bi et al. 2006)

Target plasmid. To place the six tandem repeats 19-base hairpin-binding sites of CP$_{MS2}$ (MS2 6×) in the 3′-untranslated region of pri-miR163, pri-miR163 was amplified with the *Eco*RI–*Xho*I and *Bam*HI recognition sites attached at either end, and then introduced into compatibly restricted sites of a pSL-MS2-6× plasmid (Bertrand et al. 1998). The primers used for PCR were pri-miR163 3′ fw and pri-miR163 5′ rv. The *Xho*I–*Spe*I fragment covering the pri-miR163 plus MS2 6× coding regions was inserted into a pTA7002 vector under a DEX-inducible promoter (Aoyama and Chua 1997) to obtain pri-mi163:MS2 6x-pTA7002.

CP$_{MS2}$. The coat protein of the MS2 coding sequence without the original termination codon was amplified from p14-MS2:GFP (Bertrand et al. 1998), using primers CP$_{MS2}$fw and CP$_{MS2}$rv, by PCR and subcloned into p-ENTR D-TOPO vector (Invitrogen). The resulting CP$_{MS2}$-pENTR was linearized by *Mlu*I, and subcloned into Venus-pTA7002^{GW}(C) and mCherry-pTA7002^{GW}(C) by LR reaction to obtain CP$_{MS2}$:Venus and CP$_{MS2}$:mCherry.

Nucleolin, coilin and SmD3, SmB marker plasmids

AtNUC-L2 is a homolog of human and yeast nucleolin, and localizes in the nucleolus (Pontvianne et al. 2007). We constructed AtNUC-L2 protein, C-terminally fused with mCherry, which is an improved monomeric red fluorescent protein (mRFP; Shaner et al. 2004). Coilin is a distant homolog of the vertebrate coilin gene (At1g13030) and was previously named Atcoilin(Collier et al. 2006). SmD3 is also a marker protein of CB (Li et al. 2006).

Agroinfiltration

Three-month-old *N. benthamiana* plants and *Agrobacterium tumefaciens* strain GV3101 were used for infiltration experiments. Agrobacterium culture and infiltration were performed as described previously (Llave et al. 2000). Each Agrobacterium culture was infiltrated at a density of $OD_{600} = 0.6$, except that for DCL1 where a density of $OD_{600} = 0.8$ was used. For induction of DCL1 expression, 30 μM DEX (Wako, Osaka, Japan) was sprayed onto the plants at 24 h after Agroinfiltration in a clear plastic bag.

Co-immunoprecipitation assay

At 48 h after Agroinfiltration, leaves of *N. benthamiana* were ground in liquid nitrogen and homogenized in three volumes of extraction buffer (50 mM Tris–HCl at pH 8.0, 150 mM NaCl, 0.5% Triton X-100, 0.2% 2-mercaptoethanol, 5% glycerol, complete proteinase inhibitor cocktail; Roche, Indianapolis, IN, USA) using a mortar and pestle. Cell debris was pelleted by centrifugation for 15 min at 15,000 r.p.m. The supernatant (1 ml) was incubated with 6 µl of monoclonal anti-HA–agarose conjugate (clone HA-7; Sigma Aldrich, St Louis, MO, USA) for 2 h. The immune complexes were then centrifuged and washed three times in 1 ml of phosphate-buffered saline [PBS; 0.1 M NaCl, 90 mM sodium phosphate (pH 7.0)]. The volume was reduced to 60 µl using a micropipet, and 4 vols. of sample buffer were added, followed by incubation at 65°C for 10 min.

Protein samples were analyzed on 7.5% SDS–polyacrylamide gels and transferred to Immobilon-P Transfer Membrane (Millipore, Billerica, MA, USA). Monoclonal anti-myc or anti-HA (Sigma Aldrich) mouse antibodies were used as the primary antibody, and peroxidase-conjugated anti-mouse immunoglobulins antibody (GE Healthcare, Piscataway, NJ, USA) was used as the secondary antibody. Bands were visualized by the enhanced chemiluminescence system (ECL) according to the manufacturer's instructions (GE Healthcare).

Fluorescent microscopy

The fluorescence imaging workstation for FRET imaging was an inverted fluorescence microscope equipped with a cooled CCD camera and filters, as described previously (Honda et al. 2004). FRET analysis was carried out as described previously (Honda et al. 2004).

For BiFC imaging, the fluorescence imaging workstation consisted of an Olympus IX71 inverted microscope equipped with a 40× oil objective UplanApo lens (NA 1.00; Olympus, Tokyo, Japan), a cooled CCD (cooled-color-3CCD camera, HAMAMATSU Photonics, Hamamatsu City, Japan), excitation and emission filter wheels (MAC 5000, Ludl Electronic Products, Hawthorne, NY, USA) and a hydrargyrum 75 W light source. All devices were controlled by Simple PCI software (HAMAMATSU). The filter for observation of fluorescence from Venus only was an Olympus U-MNIBA3, while when Venus and Cherry were being observed the filter used was a Chroma 51019 (Chroma, Rockingham, VT, USA). The 2D images were processed digitally using Photoshop software (Adobe Systems, San Jose, CA, USA) and ImageJ software (http://rsb.info.nih.gov/ij).

Supplementary material

Supplementary material mentioned in the article is available to online subscribers at the journal website www.pcp.oxfordjournals.org.

Acknowledgments

We would like to thank Dr. Roger Tsien for kindly providing us with mRFP and mCherry, Dr. Klaus Harter for BiFC, Dr. Robert H. Singer for MS2, and Dr. Atsushi Miyawaki for Venus. We also thank Dr. Carley Fe Li for SmD3 information in relation to the Cajal body, and Professor Ichiro Uyeda for providing *N. benthamiana* plants to perform Agroinfiltration on a separate campus. This work was supported in part by Spatiotemporal Network of RNA Information Flow Grant-in-aid for scientific research, priority area, awarded by the Ministry of Education, Culture, Sports, Science, and Technology of Japan (to Y.W.)

References

Allen, E., Xie, Z., Gustafson, A.M., Sung, G.H., Spatafora, J.W. and Carrington, J.C. (2004) Evolution of microRNA genes by inverted duplication of target gene sequences in *Arabidopsis thaliana*. *Nat. Genet.* 36: 1282–1290.

Aoyama, T. and Chua, N.H. (1997) A glucocorticoid-mediated transcriptional induction system in transgenic plants. *Plant J.* 11: 605–612.

Bertrand, E., Chartrand, P., Schaefer, M., Shenoy, S.M., Singer, R.H. and Long, R.M. (1998) Localization of ASH1 mRNA particles in living yeast. *Mol. Cell* 2: 437–445.

Bi, J., Tsai, N.P., Lin, Y.P., Loh, H.H. and Wei, L.N. (2006) Axonal mRNA transport and localized translational regulation of kappa-opioid receptor in primary neurons of dorsal root ganglia. *Proc. Natl Acad. Sci. USA* 103: 19919–19924.

Bracha-Drori, K., Shichrur, K., Katz, A., Oliva, M., Angelovici, R., Yalovsky, S. and Ohad, N. (2004) Detection of protein–protein interactions in plants using bimolecular fluorescence complementation. *Plant J.* 40: 419–427.

Cioce, M. and Lamond, A.I. (2005) Cajal bodies: a long history of discovery. *Annu. Rev. Cell Dev. Biol.* 21: 105–131.

Citovsky, V., Lee, L.Y., Vyas, S., Glick, E., Chen, M.H., Vainstein, A., Gafni, Y., Gelvin, S.B. and Tzfira, T. (2006) Subcellular localization of interacting proteins by bimolecular fluorescence complementation in planta. *J. Mol. Biol.* 362: 1120–1131.

Collier, S., Pendle, A., Boudonck, K., van Rij, T., Dolan, L. and Shaw, P. (2006) A distant coilin homologue is required for the formation of Cajal bodies in Arabidopsis. *Mol. Biol. Cell* 17: 2942–2951.

Dixit, R., Cyr, R. and Gilroy, S. (2006) Using intrinsically fluorescent proteins for plant cell imaging. *Plant J.* 45: 599–615.

Fang, Y. and Spector, D.L. (2007) Identification of nuclear dicing bodies containing proteins for microRNA biogenesis in living Arabidopsis plants. *Curr. Biol.* 17: 818–823.

Han, M.H., Goud, S., Song, L. and Fedoroff, N. (2004) The Arabidopsis double-stranded RNA-binding protein HYL1 plays a role in microRNA-mediated gene regulation. *Proc. Natl Acad. Sci. USA* 101: 1093–1098.

Hiraguri, A., Itoh, R., Kondo, N., Nomura, Y., Aizawa, D., Murai, Y., Koiwa, H., Seki, M., Shinozaki, K. and Fukuhara, T. (2005) Specific interactions between Dicer-like proteins and HYL1/DRB-family dsRNA-binding proteins in *Arabidopsis thaliana*. *Plant Mol Biol.* 57: 173–188.

Honda, K., Yanai, H., Mizutani, T., Negishi, H., Shimada, N., Suzuki, N., Ohba, Y., Takaoka, A., Yeh, W.C. and Taniguchi, T. (2004) Role of a transductional–transcriptional processor complex involving MyD88 and IRF-7 in Toll-like receptor signaling. *Proc. Natl Acad. Sci. USA* 101: 15416–15421.

Hu, C.D. and Kerppola, T.K. (2003) Simultaneous visualization of multiple protein interactions in living cells using multicolor fluorescence complementation analysis. *Nature Biotechnol.* 21: 539–545.

Jones-Rhoades, M.W., Bartel, D.P. and Bartel, B. (2006) MicroRNAs and their regulatory roles in plants. *Annu. Rev. Plant Biol.* 57: 19–53.

Kurihara, Y., Yuasa, T. and Watanabe, Y. (2006) The interaction between DCL1 and HYL1 is important for efficient and precise processing of pri-miRNA in plant microRNA biogenesis. *RNA* 12: 206–212.

Kurihara, Y. and Watanabe, Y. (2004) Arabidopsis micro-RNA biogenesis through Dicer-like 1 protein functions. *Proc. Natl Acad. Sci. USA* 101: 12753–12758.

Landthaler, M., Yalcin, A. and Tuschl, T. (2004) The human DiGeorge syndrome critical region gene 8 and its *D. melanogaster* homolog are required for miRNA biogenesis. *Curr. Biol.* 14: 2162–2167.

Li, C.F., Pontes, O., El-Shami, M., Henderson, I.R., Bernatavichute, Y.V., Chan, S.W., Lagrange, T., Pikaard, C.S. and Jacobsen, S.E. (2006) An ARGONAUTE4-containing nuclear processing center colocalized with Cajal bodies in *Arabidopsis thaliana*. *Cell* 126: 93–106.

Lim, L.P., Glasner, M.E., Yekta, S., Burge, C.B. and Bartel, D.P. (2003) Vertebrate microRNA genes. *Science* 299: 1540.

Liu, X., Jiang, F., Kalidas, S., Smith, D. and Liu, Q. (2006) Dicer-2 and R2D2 coordinately bind siRNA to promote assembly of the siRISC complexes. *RNA* 12: 1514–1520.

Llave, C., Kasschau, K.D. and Carrington, J.C. (2000) Virus-encoded suppressor of posttranscriptional gene silencing targets a maintenance step in the silencing pathway. *Proc. Natl Acad. Sci. USA* 97: 13401–13406.

Lu, C. and Fedoroff, N. (2000) A mutation in the Arabidopsis HYL1 gene encoding a dsRNA binding protein affects responses to abscisic acid, auxin, and cytokinin. *Plant Cell* 12: 2351–2366.

Nagai, T., Ibata, K., Park, E.S., Kubota, M., Mikoshiba, K. and Miyawaki, A. (2002) A variant of yellow fluorescent protein with fast and efficient maturation for cell-biological applications. *Nature Biotechnol.* 20: 87–90.

Park, W., Li, J., Song, R., Messing, J. and Chen, X. (2002) CARPEL FACTORY, a Dicer homolog, and HEN1, a novel protein, act in microRNA metabolism in *Arabidopsis thaliana*. *Curr. Biol.* 12: 1484.

Pontvianne, F., Matia, I., Douet, J., Tourmente, S., Medina, F.J., Echeverria, M. and Saez-Vasquez, J. (2007) Characterization of AtNUC-L1 reveals a central role of nucleolin in nucleolus organization and silencing of AtNUC-L2 gene in Arabidopsis. *Mol. Biol. Cell* 18: 369–379.

Saito, K., Ishizuka, A., Siomi, H. and Siomi, M.C. (2005) Processing of pre-microRNAs by the Dicer-1–Loquacious complex in *Drosophila* cells. *PLoS Biol.* 3: e235.

Sawano, A. and Miyawaki, A. (2000) Directed evolution of green fluorescent protein by a new versatile PCR strategy for site-directed and semi-random mutagenesis. *Nucleic Acids Res.* 28: E78.

Schauer, S.E., Jacobsen, S.E., Meinke, D.W. and Ray, A. (2002) DICER-LIKE1: blind men and elephants in Arabidopsis development. *Trends Plant Sci.* 7: 487–491.

Shaner, N.C., Campbell, R.E., Steinbach, P.A., Giepmans, B.N., Palmer, A.E. and Tsien, R.Y. (2004) Improved monomeric red, orange and yellow fluorescent proteins derived from Discosoma sp. red fluorescent protein. *Nature Biotechnol.* 22: 1567–1572.

Shaw, P.J. and Brown, J.W. (2004) Plant nuclear bodies. *Curr. Opin. Plant Biol.* 7: 614–620.

Song, L., Han, M.H., Lesicka, J. and Fedoroff, N. (2007) Arabidopsis primary microRNA processing proteins HYL1 and DCL1 define a nuclear body distinct from the Cajal body. *Proc. Natl Acad. Sci. USA* 104: 5437–5442.

Vazquez, F., Gasciolli, V., Crete, P. and Vaucheret, H. (2004) The nuclear dsRNA binding protein HYL1 is required for microRNA accumulation and plant development, but not posttranscriptional transgene silencing. *Curr. Biol.* 14: 346–351.

Voinnet, O., Rivas, S., Mestre, P. and Baulcombe, D. (2003) An enhanced transient expression system in plants based on suppression of gene silencing by the p19 protein of tomato bushy stunt virus. *Plant J.* 33: 949–956.

Walter, M., Chaban, C., Schutze, K., Batistic, O., Weckermann, K., et al. (2004) Visualization of protein interactions in living plant cells using bimolecular fluorescence complementation. *Plant J.* 40: 428–438.

Wu, F., Yu, L., Cao, W., Mao, Y., Liu, Z. and He, Y. (2007) The N-terminal double-stranded RNA binding domains of Arabidopsis HYPONASTIC LEAVES1 are sufficient for pre-microRNA processing. *Plant Cell* 19: 914–925.

Yang, L., Liu, Z., Lu, F., Dong, A. and Huang, H. (2006) SERRATE is a novel nuclear regulator in primary microRNA processing in Arabidopsis. *Plant J.* 47: 841–850.

(Received July 11, 2007; Accepted July 25, 2007)